Topological insulators and higher-order topological insulators from gauge-invariant one-dimensional lines

Heqiu Li and Kai Sun
Department of Physics, University of Michigan, Ann Arbor, Michigan 48109, USA

(Received 14 April 2020; accepted 22 July 2020; published 4 August 2020)

In this paper, we study the interplay between symmetry and topology with a focus on the Z_2 topological index of two-dimensional and three-dimensional (2D/3D) topological insulators and high-order topological insulators. We show that in the presence of either a two-fold-rotational symmetry or a mirror symmetry, a gauge-invariant quantity can be defined for arbitrary one-dimensional (1D) lines in the Brillouin zone. Such 1D quantities provide a new pathway to compute the Z_2 index of topological insulators. In contrast to the generic setup, where the Z_2 index generally involves 2D planes in the Brillouin zone with a globally defined smooth gauge, this 1D approach only involves some 1D lines in the Brillouin zone without requiring a global gauge. Such a simplified approach can be used in any time-reversal invariant insulators with a two-fold crystalline symmetry, which can be found in 30 of the 32 point groups. In addition, this 1D quantity can be further generalized to higher-order topological insulators to compute the magnetoelectric polarization P_3.

DOI: 10.1103/PhysRevB.102.085108

I. INTRODUCTION

In the study of topological states of matter, strong interplays between symmetry and topology have long been known to play an important role. In general, such interplays can be largely classified into two categories: (1) some symmetries are essential for the definition of a topological index, while (2) some other symmetries, although not essential, can provide an easy access to the topological index. For example, the time-reversal symmetry T is essential for the definition of the Z_2 index of topological insulators (TIs) [1–7]. The space-inversion symmetry I, in contrast, is not necessary for the Z_2 index, but its presence can dramatically simplify the calculation of this index. Without the space-inversion symmetry, it generally requires information about the two-dimensional (2D) planes in the Brillouin zone to determine the value of the Z_2 index, but in the presence of space inversion, it only requires parity eigenvalues at a few discrete momentum points [6]. Similarly, the topological monopole charge of topological nodal line semimetals [8–14] requires the space-time inversion symmetry IT, and it in general needs the wave functions of the Brillouin zone to compute [11]. However, when additional (nonessential) rotation symmetries are introduced, the index can be easily computed using rotation eigenvalues at high symmetry points [12,13], similar to the fact that the Chern number can be computed by rotation eigenvalues [15]. In both examples, nonessential symmetries simplified the topological indices from relying on the entire Brillouin zone to only a few limited momentum points. In particular, because these indices often require a smooth global gauge, which is often challenging to obtain, such symmetry-induced simplification greatly reduces the complexity of the index calculation.

Similar ideas of using symmetries to simplify the calculation of topological indices have been explored extensively in various types of topological states, which have led to many intriguing results [15–30]. On the practical side, these results provide a highly efficient way to determine the topological properties of various materials and systems, independent of the microscopic details of the band structure. In addition, on the fundamental level, these efforts provide a bridge to link various topological indices/phenomena with symmetry representations at high symmetry momenta, such as the indicator theory and topological quantum chemistry [16–24].

In this study, we focus on systems where symmetries are not strong enough to allow high symmetry points to fully dictate the topological index, e.g., a Z_2 topological insulator with a C_2 point group symmetry, and try to understand the role of nonessential symmetries in these systems. We show that for an insulator with time-reversal symmetry in two or three dimensions, as long as the system has either a two-fold-rotational symmetry or a mirror symmetry, the Z_2 index can be simplified to involve only one-dimensional lines in the Brillouin zone. This result is an extension of the high-symmetry-point-based approaches (e.g., the parity criterion [6]) from zero-dimensional (0D) points to one-dimensional (1D) lines. Here, the topological index can still be simplified by the nonessential symmetry, although high-symmetry points are no longer sufficient to dictate the index. This simplification is achieved by a gauge-invariant line quantity $g(\widetilde{k_a k_b})$ that we define below. For systems with only time-reversal symmetry, this line quantity provides a gauge-invariant way of computing topological index similar to Fukui and Hatsugai [31]. In the presence of an additional two-fold-rotational or mirror symmetry, this quantity remains gauge-invariant for any 1D path in the momentum space. By exploring its connection to the Wilson loop approach [32,33], we show that this line quantity has a physical meaning that it is a measure of the relative phase of Pfaffian in the parallel transport gauge [34]. Furthermore, this quantity also provides a gauge-independent way to calculate the magnetoelectric polarization P_3 for higher-order topological insulators [35–49].

Our result also brings convenience to the calculation of Z_2 index in practice because it only requires some 1D lines in the

Brillouin zone to be evaluated, while the original definition of the Z_2 index requires a smooth gauge in higher dimensions. Thus the evaluation can be further simplified into the parity criterion if the space-inversion symmetry is present. This approach applies generically to any time-reversal-invariant insulators with a two-fold crystalline symmetry, such as a two-fold-rotation C_2, a mirror symmetry or space inversion, which can be found in 30 of all the 32 point groups, with the only exceptions being the C_3 group and the trivial group C_1. It provides the same level of simplification as the approaches based on the partial polarization [28,29], and it can be further generalized to higher-order topological insulators.

II. GAUGE-INVARIANT QUANTITY FOR ARBITRARY LINES IN THE BRILLOUIN ZONE

In this section we define a gauge-invariant line quantity $g(\widetilde{k_a k_b})$ for systems with time-reversal symmetry T and discuss some general properties of it, and in the next section we will show that with additional two-fold crystalline-symmetry-like two-fold rotation or mirror reflection, this quantity can be utilized to simplify the calculation of the Fu-Kane-Mele (FKM) Z_2 index [1–3], although the eigenvalues of the two-fold symmetry are insufficient to determine the index. For an arbitrary path $\widetilde{k_a k_b}$ in the Brillouin zone (BZ) that connects momenta k_a and k_b, we can define $g(\widetilde{k_a k_b})$ as

$$
\begin{aligned}
g(\widetilde{k_a k_b}) &= \frac{\mathrm{Pf}[M(k_b)]}{\mathrm{Pf}[M(k_a)]}\det[W(k_a,k_b)],\\
W_{mn}(k_a,k_b) &= \langle u_m(k_a)|\prod_{k_i\in\widetilde{k_a k_b}}^{k_a\leftarrow k_b} P_{k_i}|u_n(k_b)\rangle,\\
M_{mn}(k) &= \langle u_m(k)|T|u_n(k)\rangle. \qquad (1)
\end{aligned}
$$

Here Pf refers to Pfaffian, m,n refer to occupied bands, $P_k=\sum_{m\in\mathrm{occ}}|u_m(k)\rangle\langle u_m(k)|$ is the projection operator to occupied bands and the product is path-ordered along $\widetilde{k_a k_b}$. Time-reversal T acts on wave function $|u_n(k)\rangle$ as a unitary operator times complex conjugation. The gauge invariance of $g(k_a,k_b)$ comes from the fact that for a general gauge transformation $|u_m(k)\rangle\to U_{nm}(k)|u_n(k)\rangle$, $\mathrm{Pf}[M(k)]$ changes to $\mathrm{Pf}[M(k)]\det[U(k)]^*$, and $\det[W(k_a,k_b)]$ will be multiplied by $\det[U(k_a)]^*\det[U(k_b)]$, which cancels the change in the Pfaffian. More details are shown in Appendix A. Aside from the Pfaffian part, Eq. (1) is the determinant of the Wilson line at path $\widetilde{k_a k_b}$. The determinant of a Wilson line is gauge-dependent in general, contrary to a closed Wilson loop [32,33]. The Pfaffian $\mathrm{Pf}[M(k)]$ is gauge-dependent as well, but Eq. (1) shows the combination of the two is gauge-invariant and thus smooth in any gauge. In the special case when $\widetilde{k_a k_b}$ is taken to be the straight line connecting time-reversal invariant momenta (TRIM), for example, $k_a=\Gamma=(0,0,0)$ and $k_b=X=(\pi,0,0)$, Eq. (1) coincide with the exponential of the partial polarization ν_{1D} [2,26–29]:

$$
\begin{aligned}
\nu_{1D} &= \frac{1}{\pi}\left[\int_\Gamma^X dk\,\mathrm{Tr}\,A(k)+i\log\frac{\mathrm{Pf}[\omega(X)]}{\mathrm{Pf}[\omega(\Gamma)]}\right] \mod 2\\
&= \frac{1}{\pi}i\log[g(\overline{\Gamma X})] \mod 2. \qquad (2)
\end{aligned}
$$

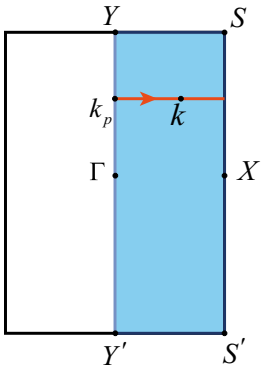

FIG. 1. The Brillouin zone for 2D insulator with time-reversal symmetry. τ is represented by the shaded area enclosed by $SYY'S'$.

Here $A(k)$ is the Berry connection and $\omega_{mn}(k)=\langle u_m(-k)|T|u_n(k)\rangle$, and we utilized the fact that ω and M coincide at time-reversal invariant momenta [2] due to the periodicity of $|u_n(k)\rangle$. For a general path $\widetilde{k_a k_b}$, $g(\widetilde{k_a k_b})$ has a physical meaning that it is a measure of the relative phase between the Pfaffian at k_a and k_b in the parallel transport gauge. To illustrate this point, we define the parallel transport gauge [34] at path $\widetilde{k_a k_b}$ so that for each $k\in\widetilde{k_a k_b}$,

$$
|u_m(k)\rangle = \prod_{k_i\in\widetilde{k k_a}}^{k\leftarrow k_a} P_{k_i}|u_m(k_a)\rangle. \qquad (3)
$$

Here the product is path-ordered from k_a to k along $\widetilde{k_a k_b}$. With this gauge choice along the path, the determinant part in $g(\widetilde{k_a k_b})$ becomes unity, leading to

$$
g(\widetilde{k_a k_b}) = \frac{\mathrm{Pf}[M(k_b)]}{\mathrm{Pf}[M(k_a)]}. \qquad (4)
$$

Hence $g(\widetilde{k_a k_b})$ represents the ratio between the Pfaffian $\mathrm{Pf}[M]$ at k_b and k_a in the parallel transport gauge. This interpretation is useful, because the topological index is related to the winding of the phase of Pfaffian. For example, in a 2D system as shown in Fig. 1, the FKM Z_2 index is given by [1,2]

$$
\nu_{2D} = \frac{1}{2\pi i}\oint_{\partial\tau} dk\cdot\nabla\log\mathrm{Pf}[M(k)]. \qquad (5)
$$

Here τ is the area enclosed by $SYY'S'$ and $\partial\tau$ is its boundary. The Pfaffian itself is gauge-dependent, making it challenging to track its phase, therefore the evaluation of Eq. (5) implicitly requires a smooth gauge on τ. The quantity $g(\widetilde{k_a k_b})$ is naturally gauge-invariant, therefore with the interpretation in Eq. (4) it provides a convenient way to bypass the gauge issue and track the phase of Pfaffian.

Now we will show that ν_{2D} can be rewritten in terms of the gauge-invariant quantity g. From now on it is sufficient to restrict the path $\widetilde{k_a k_b}$ to be the straight line $\overline{k_a k_b}$ connecting k_a and k_b and define

$$
\begin{aligned}
g(k_a,k_b) &= g(\overline{k_a k_b})\\
&= \frac{\mathrm{Pf}[M(k_b)]}{\mathrm{Pf}[M(k_a)]}\det\left[\langle u_m(k_a)|\prod_{k_i\in\overline{k_a k_b}}^{k_a\leftarrow k_b} P_{k_i}|u_n(k_b)\rangle\right]. \qquad (6)
\end{aligned}
$$

We construct a parallel transport gauge on τ as follows [34]. First, find a smooth gauge along straight line $\overline{YY'}$. This can always be done by, for example, parallel transport from Y' upwards to Y, then perform a unitary transformation for the wave functions at each momentum along the path $\overline{YY'}$ to recover the periodic condition between Y and Y'. Then for each $k \in \tau$, denote its projection to $\overline{YY'}$ as k_p such that $\overline{k_p k}$ is parallel to $\overline{YS}$, as shown in Fig. 1. The parallel transport gauge is defined by setting the wave function at k to be

$$|u_m(k)\rangle = \prod_{k_i \in \overline{k_p k}}^{k \leftarrow k_p} P_{k_i} |u_m(k_p)\rangle. \tag{7}$$

The gauge constructed in this way is smooth on τ and satisfies the periodic boundary condition between $\overline{YS}$ and $\overline{Y'S'}$ because the wave function at $\overline{YS}$ and $\overline{Y'S'}$ are parallel transported from the same set of wave functions at Y and Y'. For each $k_p \in \overline{YY'}$, we have $k_p + \pi\hat{x} \in \overline{SS'}$ and Eq. (4) implies

$$g(k_p, k_p + \pi\hat{x}) = \frac{\mathrm{Pf}[M(k_p + \pi\hat{x})]}{\mathrm{Pf}[M(k_p)]}. \tag{8}$$

This relation provides a way to reformulate the Z_2 index ν_{2D} in terms of g. Define $\bar{g}(k) = g(k, k + \pi\hat{x})$, then Eq. (5) becomes

$$\begin{aligned} \nu_{2\mathrm{D}} &= \frac{1}{2\pi i}\left(\int_{S'}^{S} - \int_{Y'}^{Y}\right) dk \cdot \nabla \log \mathrm{Pf}[M(k)] \\ &= \frac{1}{2\pi i}\int_{Y'}^{Y} dk \cdot \nabla \log \frac{\mathrm{Pf}[M(k + \pi\hat{x})]}{\mathrm{Pf}[M(k)]} \\ &= \frac{1}{2\pi i}\int_{Y'}^{Y} dk \cdot \nabla \log \bar{g}(k). \end{aligned} \tag{9}$$

Here the final integral is along a time-reversal-invariant path that connects Y, Γ and Y'. Equation (9) shows that $\nu_{2\mathrm{D}}$ can be expressed in terms of the line quantity g. Although Eq. (9) is derived in the specific parallel transport gauge, the gauge-invariance of g implies that this formula is valid in any gauge. This means that the above construction of the smooth parallel transport gauge is only a conceptual step which is never needed in a real calculation. Importantly, the evaluation of g itself does not require a smooth gauge to begin with. In practice, to evaluate ν_{2D} from Eq. (9), all we need is to make a discrete mesh of k points in τ with randomly selected phase for each wave function, and by definition in Eq. (6) the function $\bar{g}(k) = g(k, k + \pi\hat{x})$ will be smooth in k, which can lead to a well-defined result in Eq. (9). This formalism is important for our later application to higher-order topological insulators. Up to now Eq. (9) required only time-reversal symmetry, which is the least requirement in symmetry to protect the FKM Z_2 topological index.

III. TOPOLOGICAL INSULATORS WITH TWO-FOLD CRYSTALLINE SYMMETRIES IN ADDITION TO TIME-REVERSAL SYMMETRY

We will show that if 2D or 3D time-reversal-invariant topological insulators (TIs) have an additional two-fold crystalline symmetry, for example, two-fold rotation C_2 or mirror σ, the line quantity g defined above in Eqs. (1) or Eq. (6) can simplify the FKM Z_2 index ν to involve only one-dimensional lines of

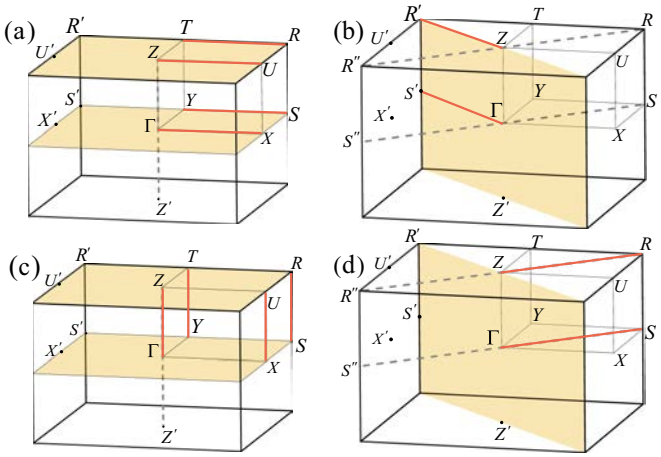

FIG. 2. The plot of a 3D Brillouin zone. The red lines denote the one-dimensional subspace that is needed to evaluate the FKM strong Z_2 index in Eqs. (15) and (18). (a) System with a C_2 symmetry along $\hat{z}$ direction. The colored planes are the C_2T invariant planes. (b) System with a C_2 symmetry along $\hat{x} + \hat{y}$ direction. There is only one C_2T invariant plane. (c) System with a mirror plane perpendicular to $\hat{z}$. (d) System with a mirror plane perpendicular to $\hat{x} + \hat{y}$.

the BZ. Note that the eigenvalues of the spacial symmetry C_2 or σ at high symmetry momenta are not sufficient to determine the Z_2 index because for a spin one-half system C_2 or σ has eigenvalues $\pm i$ and the two bands in each Kramers pair have opposite eigenvalues of C_2 or σ. Therefore, at any C_2-invariant momentum there are always a half of valence bands with C_2 or mirror eigenvalue $+i$ and the other half with eigenvalue $-i$ no matter ν is trivial or not. Hence spacial symmetry eigenvalues themselves are insufficient to determine the topological index.

A. Systems with additional two-fold rotational symmetry

When the system has additional spacial symmetries, the line quantity $g(k_a, k_b)$ has a useful property that if a point k in the BZ is transformed to Ck under a symmetry operator C which commutes with time-reversal T, then depending on whether C is unitary or antiunitary, $g(k_a, k_b)$ in Eq. (6) satisfies

$$\begin{aligned} g(Ck_a, Ck_b) &= g(k_a, k_b), \quad \text{if C is unitary,} \\ g(Ck_a, Ck_b) &= g(k_a, k_b)^*, \quad \text{if C is antiunitary.} \end{aligned} \tag{10}$$

This property comes from the transformation properties of the Pfaffian and the Wilson line operator. We give a detailed proof of this property in the Appendix. This property is important in evaluating $g(k_a, k_b)$ at symmetry-related lines in the BZ. Now we consider systems with a two-fold rotational symmetry C_2 in additional to time-reversal T. The combined operator C_2T is also a symmetry of the system which acts on the momentum space like a mirror, therefore there are C_2T invariant planes in the BZ. Suppose there are two such planes that include all eight time-reversal-invariant momenta (TRIM) as in Fig. 2(a), where the C_2 axis is along z direction and C_2T-invariant planes are colored in yellow. If k_a, k_b are taken inside one of the C_2T invariant planes, then Eq. (10) shows $g(k_a, k_b) = g(C_2Tk_a, C_2Tk_b)^* = g(k_a, k_b)^*$ so that $g(k_a, k_b)$ is real because C_2T is antiunitary. If k_a, k_b are taken to be TRIM, then $g(k_a, k_b)$ should have a magnitude of 1 because the M

matrices in Eq. (6) are unitary at TRIM. These two conditions quantize $g(K_1, K_2)$ to ± 1, where K_1, K_2 are TRIM in the same C_2T-invariant plane. Furthermore, as in Eq. (2), $g(K_1, K_2)$ is related to the partial polarization ν_{1D}:

$$\nu_{1D}(K_1, K_2) = \frac{1}{\pi}\left[\int_{K_1}^{K_2} dk \,\mathrm{Tr}\, A(k) + i \log \frac{\mathrm{Pf}[\omega(K_2)]}{\mathrm{Pf}[\omega(K_1)]}\right] \times \mod 2,$$
$$g(K_1, K_2) = e^{i\pi \nu_{1D}(K_1, K_2)} = \pm 1. \tag{11}$$

It has been shown in Ref. [29] that the FKM Z_2 index for a 2D system is equivalent to the difference between the 1D partial polarization ν_{1D} at two pairs of TRIM:

$$\nu_{2D}(k_z = 0) = \nu_{1D}(\Gamma, X) - \nu_{1D}(Y, S) \mod 2,$$
$$\nu_{2D}(k_z = \pi) = \nu_{1D}(Z, U) - \nu_{1D}(T, R) \mod 2. \tag{12}$$

The FKM strong Z_2 index in three dimensions is given by $\nu_{3D} = \nu_{2D}(k_z = 0) - \nu_{2D}(k_z = \pi) \mod 2$. Combining with Eq. (11) we have

$$(-1)^{\nu_{3D}} = g(\Gamma, X)g(Y, S)g(Z, U)g(T, R) \tag{13}$$

Therefore the 3D strong Z_2 index is simplified by the line quantity $g(k_a, k_b)$ so that it involves only a 1D subspace of the BZ.

Equation (13) assumes that all the eight TRIM are included in some C_2T invariant planes, which is not always true for a general C_2 rotation. For example, if the C_2 axis is along the direction $\hat{x} + \hat{y}$ rather than $\hat{z}$ for the same Brillouin zone as in Fig. 2(b), there is only one C_2T-invariant plane S_1 passing through Γ, S', R', Z. Denote the other time-reversal-invariant plane passing through X, Y, T, U as S_2, Then $\nu_{3D} = \nu_{2D}(S_1) - \nu_{2D}(S_2) \mod 2$. We show that $\nu_{2D}(S_2)$ must vanish due to the C_2 symmetry. Denote the midpoint of $\overline{XY}$ as M. Since C_2 is unitary, from Eq. (10) we have $g(X, M) = g(C_2X, C_2M) = g(Y, M) = g(M, Y)^{-1}$. Therefore $g(X, Y) = g(X, M)g(M, Y) = 1$, which means the partial polarization $\nu_{1D}(X, Y)$ is quantized to 0. The same argument can be applied to $\overline{TU}$. Hence $\nu_{1D}(X, Y) = \nu_{1D}(T, U) = 0$ due to the C_2 symmetry, therefore $\nu_{2D}(S_2)$ vanishes. We present a more detailed proof of the triviality of $\nu_{2D}(S_2)$ in the Appendix using the interpretation of $g(k_a, k_b)$ as a measure of Pfaffian in the parallel transport gauge. With this result, the strong Z_2 index ν_{3D} is determined only by lines in C_2T-invariant plane S_1:

$$(-1)^{\nu_{3D}} = (-1)^{\nu_{2D}(S_1)} = g(\Gamma, S')g(Z, R'). \tag{14}$$

The above proof for Eqs. (13) and (14) for different types of C_2 axis can be unified in a general framework, which is also applicable to Brillouin zones that are not cube-shaped. There are eight TRIM $K_i, i = 1, \ldots, 8$ in a 3D BZ. Since time-reversal operator commutes with C_2, C_2 must bring one TRIM to itself or to another TRIM. For those TRIM non-invariant under C_2, let $C_2K_i = K_j$ and $C_2K_j = K_i$, then the midpoint $M = (K_i + K_j)/2$ must be invariant under C_2, and $g(K_i, M) = g(C_2K_i, C_2M) = g(K_j, M) = g(M, K_j)^{-1}$. Therefore $g(K_i, K_j) = g(K_i, M)g(M, K_j) = 1$. This fixes the partial polarization $\nu_{1D}(K_i, K_j) = 0$, which does not contribute to the strong index ν_{3D}. Therefore we only need to consider those TRIM that are also invariant under C_2. Define the C_2T-invariant subspace in the BZ by $S_{C_2T} = \{k \in BZ | C_2Tk = k + G\}$ where G is any reciprocal lattice vector, and define a set L_{C_2T} to be the set of straight paths inside S_{C_2T} such that each path $\gamma \in L_{C_2T}$ connects two C_2-invariant TRIM, different paths in L_{C_2T} do not cross with each other, and each C_2-invariant TRIM is connected by one path in L_{C_2T}. With this definition, in Figs. 2(a) and 2(b) L_{C_2T} reduces to the red lines $\{\overline{\Gamma X}, \overline{YS}, \overline{ZU}, \overline{TR}\}$ and $\{\overline{\Gamma S'}, \overline{ZR'}\}$, respectively (or equivalently $\{\overline{\Gamma Y}, \overline{XS}, \overline{ZT}, \overline{UR}\}$ and $\{\overline{\Gamma Z}, \overline{S'R'}\}$, which does not change the final result). Therefore Eqs. (13) and (14) can be unified as

$$(-1)^{\nu_{3D}} = \prod_{\gamma \in L_{C_2T}} \mathrm{Sign}[g(\gamma)]. \tag{15}$$

Here the sign function Sign is added to take account of the fact that the absolute value of $g(\gamma)$ can be smaller than 1 in a practical numerical calculation in which the projection in Eq. (6) is taken at discrete points. In this case $g(\gamma)$ is still real, and the sign of it determines the index ν_{3D}. Equation (15) shows that for any topological insulator with an additional two-fold rotational symmetry, the FKM strong Z_2 index can be computed through a well-defined one-dimensional subspace of the Brillouin zone. If there are multiple C_2 axes in the system, this simplification can be applied to any one of the C_2, independent of the presence of the other symmetries. This calculation is applicable to 2D insulators as well, which can be achieved by restricting L_{C_2T} to the 2D Brillouin zone. This method is convenient to implement in the sense that it does not require a smooth gauge because the definition of $g(\gamma)$ in Eq. (6) is gauge-independent.

B. Systems with additional mirror symmetry

For systems with a mirror symmetry σ in additional to T, a similar analysis can be applied by evaluating $g(k_a, k_b)$ in the σT-invariant subspace defined by $S_{\sigma T} = \{k \in BZ | \sigma Tk = k + G\}$. If the mirror is perpendicular to $\hat{z}$ as in Fig. 2(c), then $S_{\sigma T}$ consists of four straight paths along the $\hat{z}$ direction that pass through TRIM. Since σT is antiunitary, Eq. (10) implies $g(\Gamma, Z) = g(\sigma T\Gamma, \sigma TZ)^* = g(\Gamma, Z)^*$, therefore $g(\Gamma, Z)$ is real and quantizes to ± 1, so as $g(X, U), g(Y, T), g(S, R)$. Following the same argument as the C_2 case, we have

$$\nu_{3D} = g(\Gamma, Z)g(X, U)g(Y, T)g(S, R). \tag{16}$$

If the mirror plane is perpendicular to $\hat{x} + \hat{y}$ as in Fig. 2(d), $S_{\sigma T}$ consists of two lines $\{\overline{SS''}, \overline{RR''}\}$. The TRIM Γ, S, Z, R are invariant under the mirror symmetry σ but X', Y, U', T are not. Following the same argument, $g(X', Y)$ and $g(U', T)$ are fixed to 1 because these two points interchange under σ, therefore they do not contribute to ν_{3D}. In this case we have

$$\nu_{3D} = g(\Gamma, S)g(Z, R). \tag{17}$$

In general, similar to the C_2 case above, we can define $L_{\sigma T}$ to be the set of straight paths inside $S_{\sigma T}$ such that each path $\gamma \in L_{\sigma T}$ connects two mirror-invariant TRIM, different paths in $L_{\sigma T}$ do not cross with each other, and each mirror-invariant TRIM is connected by one path in $L_{\sigma T}$. In Figs. 2(c) and 2(d) $L_{\sigma T}$ reduces to $\{\overline{\Gamma Z}, \overline{XU}, \overline{YT}, \overline{SR}\}$ and $\{\overline{\Gamma S}, \overline{ZR}\}$, respectively. Note that in Fig. 2(d) we cannot take $\{\overline{\Gamma Z}, \overline{SR}\}$ because these lines are not inside σT invariant subspace. With this

definition, the index is written as

$$\nu_{3D} = \prod_{\gamma \in L_{\sigma T}} \mathrm{Sign}[g(\gamma)]. \tag{18}$$

Here the sign function takes account of the fact that $|g(\gamma)|$ can be smaller than 1 in a real calculation on discrete momentum points. With Eqs. (15) and (18), we developed a unified method to calculate FKM strong Z_2 topological index that requires examining only a 1D subspace of the BZ, for systems with two-fold rotation or mirror symmetry. If the system has multiple mirrors or C_2 axes, this method will work if we focus on any one of them.

Our formalism is capable of calculating the weak topological index as well because the weak index is obtained from a 2D plane in the Brillouin zone passing through four of the eight TRIM, and our line quantity g can be utilized to calculate the 2D index, as in Eq. (9). Therefore, the weak topological index can be obtained by applying Eq. (9) to the corresponding 2D plane.

It is also worthwhile to explore the situation when the system has space-inversion symmetry I in addition to T. It turns out that our method is still applicable, although the Z_2 index can be determined directly by inversion eigenvalues. In this case Eq. (10) when applied to symmetry operator IT shows that that $g(k_a, k_b)$ is real everywhere since every momentum point is invariant under IT. This implies $g(K_i, K_j)$ will be quantized to ± 1 for any pair of TRIM K_i and K_j. Therefore our method is applicable again and we have $(-1)^{\nu_{3D}} = \prod_\gamma g(\gamma)$, where the product ranges over the four lines that connect the eight TRIM.

IV. HIGHER-ORDER TOPOLOGICAL INSULATORS WITH C_4T SYMMETRY

The Pfaffian formalism that describes the FKM Z_2 index for topological insulators has recently been generalized to higher-order topological insulators [42]. We show that the line quantity $g(k_a, k_b)$ can be applied to calculate the topological index for higher-order topological insulators as well. Consider the chiral second-order topological insulator protected by C_4T symmetry. The topological index is the magnetoelectric polarization P_3, which is quantized to 0 or $\frac{1}{2}$ by C_4T symmetry, satisfying a Z_2 classification. If $P_3 = \frac{1}{2}$ the system is topological, with gapless states localized at the one-dimensional hinges, but the system remains gapped at the bulk and 2D side surfaces. Time-reversal symmetry in this system is broken, therefore the original FKM Pfaffian formalism which requires time-reversal symmetry is not applicable. However, it has been shown in Ref. [42] that with the definition of a composite operator $\Theta = \frac{C_4T + C_4^{-1}T}{\sqrt{2}}$, the topological index P_3 can be represented by a Pfaffian formula in which T is replaced by Θ:

$$2P_3 = \frac{1}{2\pi i} \oint_{\partial\tau} dk \cdot \nabla \log \mathrm{Pf}[M_\Theta(k)] \mod 2, \tag{19}$$

$$M_{\Theta,mn}(k) = \langle u_m(k)|\Theta|u_n(k)\rangle. \tag{20}$$

Here τ is the colored area in Fig. 3 and the C_4 axis is along the $\hat{z}$ direction. Equation (19) has the same form as Eq. (5) with T replaced by Θ. We can make the same replacement in the definition of $g(k_a, k_b)$ in Eq. (6) to define

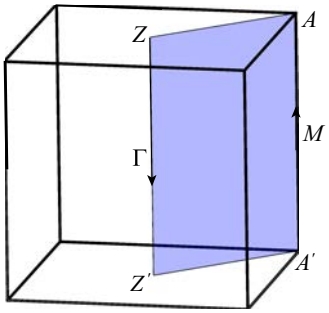

FIG. 3. The plot of a 3D Brillouin zone for higher-order topological insulator protected by C_4T symmetry. The C_4 axis is along $\hat{z}$ direction and τ is the colored area.

$$g_\Theta(k_a, k_b) = \frac{\mathrm{Pf}[M_\Theta(k_b)]}{\mathrm{Pf}[M_\Theta(k_a)]} \det\left[\langle u_m(k_a)| \prod_{k_i \in \overline{k_a k_b}}^{k_a \leftarrow k_b} P_{k_i} |u_n(k_b)\rangle\right]. \tag{21}$$

The line quantity $g_\Theta(k_a, k_b)$ defined in this way is gauge-invariant as well. Following the same procedure that lead to Eq. (9), we arrive at

$$2P_3 = \frac{1}{2\pi i} \int_{Z'}^{Z} dk \cdot \nabla \log \bar{g}_\Theta(k) \mod 2. \tag{22}$$

Here $\bar{g}_\Theta(k) = g_\Theta(k, k + \pi\hat{x} + \pi\hat{y})$ and the integral is along the straight path from Z' to Z. Therefore the magnetoelectric polarization P_3 can be expressed in terms of an integral of the line quantity $g_\Theta(k_a, k_b)$. The advantage of this method is that it involves only gauge-independent objects, therefore a smooth gauge is not needed.

V. CONCLUSION

We show that in systems where topological indices cannot be reduced to high-symmetry-point symmetry eigenvalues, certain symmetries can still help simplify the calculation of the index. With the definition of the gauge-invariant line quantity $g(k_a, k_b)$, we present a unified way to calculate the topological index by examining only 1D subspace of the Brillouin zone for systems with either C_2 or mirror symmetry in addition to time-reversal symmetry. Our method is applicable to a wide range of systems because, among all the 32 point groups, 30 of them contain such a symmetry, except for C_3 the the trivial group C_1. This approach also finds its application in higher-order topological insulators.

ACKNOWLEDGMENT

H.L. and K.S. acknowledge the support of the National Science Foundation Grant No. EFRI-1741618.

APPENDIX A: PROPERTIES OF $g(\widetilde{k_a k_b})$

Here we prove some equalities involving $g(\widetilde{k_a k_b})$ defined in Eq. (1). First we investigate the case when k_a and k_b are infinitely close to each other, denoted as k_1 and k_2. In this case we have $g(k_1, k_2) = \frac{\mathrm{Pf}[M(k_2)]}{\mathrm{Pf}[M(k_1)]} \det[W(k_1, k_2)]$ and $W(k_1, k_2)$

reduces to the overlap between the wave functions at k_1 and k_2: $W_{mn}(k_1,k_2)=\langle u_m(k_1)|u_n(k_2)\rangle$. $g(k_1,k_2)$ is invariant under gauge transformation $|u_m(k)\rangle\to U_{nm}(k)|u_n(k)\rangle$. Since under this transformation, $M_{mn}(k)=\langle u_m(k)|T|u_n(k)\rangle\to (U(k)^\dagger M(k)U(k)^*)_{mn}$, $W_{mn}(k_1,k_2)=\langle u_m(k_1)|u_n(k_2)\rangle\to (U(k_1)^\dagger W(k_1,k_2)U(k_2))_{mn}$, therefore

$$\begin{aligned}\mathrm{Pf}[M(k)]&\to \mathrm{Pf}[M(k)]\det[U(k)]^*\\ \det[W(k_1,k_2)]&\to \det[W(k_1,k_2)]\det[U(k_1)]^*\det[U(k_2)],\\ g(k_1,k_2)&=\frac{\mathrm{Pf}[M(k_2)]}{\mathrm{Pf}[M(k_1)]}\det[W(k_1,k_2)]\to g(k_1,k_2).\end{aligned}\tag{A1}$$

This completes the proof that $g(k_1,k_2)$ is gauge-invariant. For a general path $\widetilde{k_ak_b}$, divide the path by small segments (k_i,k_{i+1}) and by definition in Eq. (1), $g(\widetilde{k_ak_b})=\prod_i g(k_i,k_{i+1})$. For each small segment $g(k_i,k_{i+1})$ is gauge-invariant, therefore $g(\widetilde{k_ak_b})$ is gauge-invariant as well.

Next we prove Eq. (10). Suppose the system has an antiunitary symmetry C such that it commutes with T and it transforms momentum k to Ck, define the sewing matrix of C as

$$R_{mn}(k)=\langle u_m(Ck)|C|u_n(k)\rangle.\tag{A2}$$

Insert identity $\mathbf{1}=P_{\mathrm{occ}}(k)+P_{\mathrm{unocc}}(k)=\sum_{i\in\mathrm{occ}}|u_i(k)\rangle\langle u_i(k)|+\sum_{i\in\mathrm{unocc}}|u_i(k)\rangle\langle u_i(k)|$ to each $\mathbf{1}$ in the identity below:

$$\langle u_m(Ck)|T|u_n(Ck)\rangle=\langle u_m(Ck)|C\mathbf{1}T\mathbf{1}C^{-1}|u_n(Ck)\rangle,\tag{A3}$$

where P_{occ} and P_{unocc} are projection to the occupied and unoccupied bands, respectively, m and n belong to the occupied bands. Since $\langle u_m(Ck)|CP_{\mathrm{unocc}}(k)=0$, we can omit P_{unocc} in the insertion and get

$$\begin{aligned}\langle u_m(Ck)|T|u_n(Ck)\rangle=&\sum_{i,j\in occ}\langle u_m(Ck)|C|u_i(k)\rangle\langle u_i(k)|\\ &\times T|u_j(k)\rangle^*\langle u_j(k)|C^{-1}|u_n(Ck)\rangle,\end{aligned}\tag{A4}$$

where the conjugation is due to the fact that T and C are antiunitary. Notice that $\langle u_j(k)|C^{-1}|u_n(Ck)\rangle=\langle u_n(Ck)|C|u_j(k)\rangle$, the above equation implies

$$\begin{aligned}M(Ck)&=R(k)M(k)^*R(k)^T,\\ \mathrm{Pf}[M(Ck)]&=\det[R(k)]\,\mathrm{Pf}[M(k)]^*.\end{aligned}\tag{A5}$$

To prove Eq. (10) we still need to compute $W(Ck_1,Ck_2)$. Using $|u_m(Ck)\rangle=R^\dagger_{nm}(k)C|u_n(k)\rangle$ we get

$$\begin{aligned}W_{ij}(Ck_1,Ck_2)&=R_{in}(k_1)\langle Cu_n(k_1)|Cu_m(k_2)\rangle R^\dagger_{mj}(k_2)\rangle\\ &=R_{in}(k_1)\langle u_n(k_1)|u_m(k_2)\rangle^*R^\dagger_{mj}(k_2)\rangle,\\ \det[W(Ck_1,Ck_2)]&=\det[W(k_1,k_2)]^*\det[R(k_1)]\det[R(k_2)]^*.\end{aligned}\tag{A6}$$

Therefore when C is antiunitary we have

$$\begin{aligned}g(Ck_1,Ck_2)&=\frac{\mathrm{Pf}[M(Ck_2)]}{\mathrm{Pf}[M(Ck_1)]}\det[W(Ck_1,Ck_2)]\\ &=\frac{\mathrm{Pf}[M(k_2)]^*}{\mathrm{Pf}[M(k_1)]^*}\det[W(k_1,k_2)]^*=g(k_1,k_2)^*.\end{aligned}\tag{A7}$$

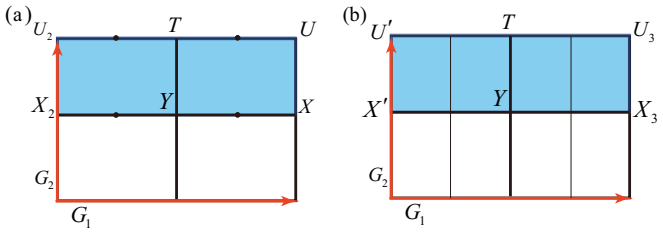

FIG. 4. The plot of time-reversal-invariant planes obtained from a cut in Figs. 2(b) and 2(d). We define the origin in these planes to be at Y. The black dots in (a) are two-fold rotation centers. The thin vertical lines in (b) are mirror planes. Note that none of these two-fold rotation centers or mirror planes pass through the origin at Y.

If C is unitary instead, Eq. (A4) will be changed to

$$\begin{aligned}\langle u_m(Ck)|T|u_n(Ck)\rangle=&\sum_{i,j\in occ}\langle u_m(Ck)|C|u_i(k)\rangle\langle u_i(k)|T|u_j(k)\rangle\\ &\times\langle u_j(k)|C^{-1}|u_n(Ck)\rangle^*,\end{aligned}\tag{A8}$$

Using $\langle u_j(k)|C^{-1}|u_n(Ck)\rangle^*=\langle u_n(Ck)|C|u_j(k)\rangle$ for unitary symmetry C, we have

$$\begin{aligned}M(Ck)&=R(k)M(k)R(k)^T,\\ \mathrm{Pf}[M(Ck)]&=\det[R(k)]\,\mathrm{Pf}[M(k)].\end{aligned}\tag{A9}$$

For $W(Ck_1,Ck_2)$, Eq. (A6) will be

$$\begin{aligned}W_{ij}(Ck_1,Ck_2)&=R_{in}(k_1)\langle Cu_n(k_1)|Cu_m(k_2)\rangle R^\dagger_{mj}(k_2)\rangle\\ &=R_{in}(k_1)\langle u_n(k_1)|u_m(k_2)\rangle R^\dagger_{mj}(k_2)\rangle,\\ \det[W(Ck_1,Ck_2)]&=\det[W(k_1,k_2)]\det[R(k_1)]\det[R(k_2)]^*.\end{aligned}\tag{A10}$$

Therefore if C is unitary we have

$$\begin{aligned}g(Ck_1,Ck_2)&=\frac{\mathrm{Pf}[M(Ck_2)]}{\mathrm{Pf}[M(Ck_1)]}\det[W(Ck_1,Ck_2)]\\ &=\frac{\mathrm{Pf}[M(k_2)]}{\mathrm{Pf}[M(k_1)]}\det[W(k_1,k_2)]=g(k_1,k_2).\end{aligned}\tag{A11}$$

A general path $\widetilde{k_ak_b}$ can be divided by small segments (k_i,k_{i+1}) so that $g(\widetilde{k_ak_b})=\prod_i g(k_i,k_{i+1})$. Eq. (10) is proved by applying Eqs. (A7) or (A11) to each segment $g(k_i,k_{i+1})$.

APPENDIX B: TRIVIALITY OF TRIM THAT ARE NOT INVARIANT UNDER C_2 OR MIRROR SYMMETRY

In this section we give a more detailed proof of the assertion that the Z_2 index $\nu_{2\mathrm{D}}$ in the time-reversal-invariant plane passing through X,Y,T,U in Fig. 2(b) and X',Y,T,U' in Fig. 2(d) are trivial. These 2D planes are shown in Fig. 4, which are obtained from a cut in Figs. 2(b) and 2(d), respectively. This proof utilizes the interpretation of the line quantity $g(\widetilde{k_ak_b})$ as a measure of Pfaffian in the parallel transport gauge.

In Fig. 4(a) the system has a two-fold rotational symmetry C_2 perpendicular to the plane which is inherited from the 3D system. However, the C_2 rotation centers are located at the black dots that bisect two TRIM. This type of C_2 operator is different from the conventional two-fold rotation that can be

realized by a 2D lattice in real space since, in that case, the rotation center in the momentum space will always locate at some TRIM. If we choose the origin to be at Y and denote the components of k along G_1 and G_2 direction as k_x and k_y, respectively, the C_2 operator at the midpoint of $\overline{XY}$ generates a transformation $(k_x, k_y) \to (G_1/2 - k_x, -k_y)$, and time-reversal generates $(k_x, k_y) \to (-k_x, -k_y)$. Therefore the combined operation C_2T gives $(k_x, k_y) \to (k_x - G_1/2, k_y)$. Define $\bar{g}(\mathbf{k}) = g(\mathbf{k}, \mathbf{k} + \mathbf{G}_2/2)$ for $\mathbf{k} \in \overline{XX_2}$, then from Eq. (10) the C_2T symmetry requires

$$\bar{g}(\mathbf{k}) = \bar{g}(\mathbf{k} + \mathbf{G}_1/2)^*,$$
$$\mathrm{Im}\log\bar{g}(\mathbf{k}) = -\mathrm{Im}\log\bar{g}(\mathbf{k} + \mathbf{G}_1/2),\ \mathbf{k} \in \overline{XX_2}. \quad \text{(B1)}$$

Denote the colored region in Fig. 4 as τ and use the same derivation that lead to Eq. (9), the Z_2 index in this plane is

$$\nu_{2D} = \frac{1}{2\pi}\mathrm{Im}\int_{X_2}^{X} d\mathbf{k}\cdot\nabla\log\bar{g}(\mathbf{k}),$$
$$\bar{g}(\mathbf{k}) = g(\mathbf{k}, \mathbf{k} + \mathbf{G}_2/2). \quad \text{(B2)}$$

From Eq. (B1), the integrand in Eq. (B2) at $\mathbf{k}$ cancels that at $\mathbf{k} + \mathbf{G}_1/2$, which leads to $\nu_{2D} = 0$. Therefore the plane has a trivial Z_2 index due to the C_2 symmetry.

In Fig. 4(b) the system has mirror planes inherited from the 3D system located at the thin vertical lines. The mirror plane to the right has the transformation $(k_x, k_y) \to (G_1/2 - k_x, k_y)$. Define $\bar{g}(\mathbf{k}) = g(\mathbf{k}, \mathbf{k} + \mathbf{G}_2/2)$ for $\mathbf{k} \in \overline{X'X_3}$, from Eq. (10) the mirror symmetry requires

$$\bar{g}(\mathbf{k}) = \bar{g}(\mathbf{G}_1/2 - \mathbf{k}). \quad \text{(B3)}$$

The Z_2 index from Eq. (9) is

$$\nu_{2D} = \frac{1}{2\pi}\mathrm{Im}\int_{X'}^{X_3} d\mathbf{k}\cdot\nabla\log\bar{g}(\mathbf{k}). \quad \text{(B4)}$$

Therefore Eq. (B3) requires the integrand at $\mathbf{k}$ to cancel that at $\mathbf{G}_1/2 - \mathbf{k}$, leading to $\nu_{2D} = 0$. Therefore the Z_2 index for this 2D plane is trivial due to the mirror symmetry.

[1] C. L. Kane and E. J. Mele, Z_2 Topological Order and the Quantum Spin Hall Effect, Phys. Rev. Lett. **95**, 146802 (2005).

[2] L. Fu and C. L. Kane, Time reversal polarization and a Z_2 adiabatic spin pump, Phys. Rev. B **74**, 195312 (2006).

[3] L. Fu, C. L. Kane, and E. J. Mele, Topological Insulators in Three Dimensions, Phys. Rev. Lett. **98**, 106803 (2007).

[4] X.-L. Qi and S.-C. Zhang, Topological insulators and superconductors, Rev. Mod. Phys. **83**, 1057 (2011).

[5] M. Z. Hasan and C. L. Kane, *Colloquium*: Topological insulators, Rev. Mod. Phys. **82**, 3045 (2010).

[6] L. Fu and C. L. Kane, Topological insulators with inversion symmetry, Phys. Rev. B **76**, 045302 (2007).

[7] X.-L. Qi, T. L. Hughes, and S.-C. Zhang, Topological field theory of time-reversal invariant insulators, Phys. Rev. B **78**, 195424 (2008).

[8] C. Fang, H. Weng, X. Dai, and Z. Fang, Topological nodal line semimetals, Chin. Phys. B **25**, 117106 (2016).

[9] T. Bzdušek and M. Sigrist, Robust doubly charged nodal lines and nodal surfaces in centrosymmetric systems, Phys. Rev. B **96**, 155105 (2017).

[10] J. Ahn, D. Kim, Y. Kim, and B.-J. Yang, Band Topology and Linking Structure of Nodal Line Semimetals with Z_2 Monopole Charges, Phys. Rev. Lett. **121**, 106403 (2018).

[11] C. Fang, Y. Chen, H.-Y. Kee, and L. Fu, Topological nodal line semimetals with and without spin-orbital coupling, Phys. Rev. B **92**, 081201(R) (2015).

[12] H. Li, C. Fang, and K. Sun, Diagnosis of topological nodal lines with nontrivial monopole charge in the presence of rotation symmetries, Phys. Rev. B **100**, 195308 (2019).

[13] Z. Song, T. Zhang, and C. Fang, Diagnosis for Nonmagnetic Topological Semimetals in the Absence of Spin-Orbital Coupling, Phys. Rev. X **8**, 031069 (2018).

[14] A. Lau and C. Ortix, Topological Semimetals in the SnTe Material Class: Nodal Lines and Weyl Points, Phys. Rev. Lett. **122**, 186801 (2019).

[15] C. Fang, M. J. Gilbert, and B. A. Bernevig, Bulk topological invariants in noninteracting point group symmetric insulators, Phys. Rev. B **86**, 115112 (2012).

[16] B. Bradlyn, L. Elcoro, J. Cano, M. G. Vergniory, Z. Wang, C. Felser, M. I. Aroyo, and B. A. Bernevig, Topological quantum chemistry, Nature **547**, 298 (2017).

[17] H. C. Po, A. Vishwanath, and H. Watanabe, Symmetry-based indicators of band topology in the 230 space groups, Nat. Commun. **8**, 50 (2017).

[18] J. Kruthoff, J. de Boer, J. van Wezel, C. L. Kane, and R.-J. Slager, Topological Classification of Crystalline Insulators through Band Structure Combinatorics, Phys. Rev. X **7**, 041069 (2017).

[19] E. Khalaf, H. C. Po, A. Vishwanath, and H. Watanabe, Symmetry Indicators and Anomalous Surface States of Topological Crystalline Insulators, Phys. Rev. X **8**, 031070 (2018).

[20] S. Ono and H. Watanabe, Unified understanding of symmetry indicators for all internal symmetry classes, Phys. Rev. B **98**, 115150 (2018).

[21] Z. Song, T. Zhang, Z. Fang, and C. Fang, Quantitative mappings between symmetry and topology in solids, Nat. Commun. **9**, 3530 (2018).

[22] T. Zhang, Y. Jiang, Z. Song, H. Huang, Y. He, Z. Fang, H. Weng, and C. Fang, Catalogue of topological electronic materials, Nature **566**, 475 (2019).

[23] F. Tang, H. C. Po, A. Vishwanath, and X. Wan, Comprehensive search for topological materials using symmetry indicators, Nature **566**, 486 (2019).

[24] M. G. Vergniory, L. Elcoro, C. Felser, N. Regnault, B. A. Bernevig, and Z. Wang, A complete catalog of high-quality topological materials, Nature **566**, 480 (2019).

[25] A. Alexandradinata and B. A. Bernevig, Berry-phase description of topological crystalline insulators, Phys. Rev. B **93**, 205104 (2016).

[26] A. Lau, J. van den Brink, and C. Ortix, Topological mirror insulators in one dimension, Phys. Rev. B **94**, 165164 (2016).

[27] G. van Miert and C. Ortix, Excess charges as a probe of one-dimensional topological crystalline insulating phases, Phys. Rev. B **96**, 235130 (2017).

[28] S. H. Kooi, G. van Miert, and C. Ortix, Classification of crystalline insulators without symmetry indicators: Atomic and fragile topological phases in twofold rotation symmetric systems, Phys. Rev. B **100**, 115160 (2019).

[29] J. Kruthoff, J. de Boer, and J. van Wezel, Topology in time-reversal symmetric crystals, Phys. Rev. B **100**, 075116 (2019).

[30] J. Yu, Z.-D. Song, and C.-X. Liu, Gapless Criterion for Crystals from Effective Axion Field, Phys. Rev. Lett. **125**, 036401 (2020).

[31] T. Fukui and Y. Hatsugai, Quantum spin Hall effect in three dimensional materials: Lattice computation of Z_2 topological invariants and its application to Bi and Sb, J. Phys. Soc. Jpn. **76**, 053702 (2007).

[32] R. Yu, X. L. Qi, A. Bernevig, Z. Fang, and X. Dai, Equivalent expression of $\mathbb{Z}_2$ topological invariant for band insulators using the non-Abelian Berry connection, Phys. Rev. B **84**, 075119 (2011).

[33] A. Alexandradinata, X. Dai, and B. A. Bernevig, Wilson-loop characterization of inversion-symmetric topological insulators, Phys. Rev. B **89**, 155114 (2014).

[34] A. A. Soluyanov and D. Vanderbilt, Smooth gauge for topological insulators, Phys. Rev. B **85**, 115415 (2012).

[35] W. A. Benalcazar, B. A. Bernevig, and T. L. Hughes, Quantized electric multipole insulators, Science **357**, 61 (2017).

[36] W. A. Benalcazar, B. A. Bernevig, and T. L. Hughes, Electric multipole moments, topological multipole moment pumping, and chiral hinge states in crystalline insulators, Phys. Rev. B **96**, 245115 (2017).

[37] F. Schindler, A. M. Cook, M. G. Vergniory, Z. Wang, S. S. P. Parkin, B. A. Bernevig, and T. Neupert, Higher-order topological insulators, Sci. Adv **4**, eaat0346 (2018).

[38] F. Schindler, Z. Wang, M. G. Vergniory, A. M. Cook, A. Murani, S. Sengupta, A. Y. Kasumov, R. Deblock, S. Jeon, I. Drozdov, H. Bouchiat, S. Guéron, A. Yazdani, B. A. Bernevig, and T. Neupert, Higher-order topology in bismuth, Nat. Phys. **14**, 918 (2018).

[39] Z. Song, Z. Fang, and C. Fang, $(d-2)$-Dimensional Edge States of Rotation Symmetry Protected Topological States, Phys. Rev. Lett. **119**, 246402 (2017).

[40] J. Langbehn, Y. Peng, L. Trifunovic, F. von Oppen, and P. W. Brouwer, Reflection-Symmetric Second-Order Topological Insulators and Superconductors, Phys. Rev. Lett. **119**, 246401 (2017).

[41] J. Ahn and B.-J. Yang, Symmetry representation approach to topological invariants in $C_{2z}T$-symmetric systems, Phys. Rev. B **99**, 235125 (2019).

[42] H. Li and K. Sun, Pfaffian Formalism for Higher-Order Topological Insulators, Phys. Rev. Lett. **124**, 036401 (2020).

[43] M. Geier, L. Trifunovic, M. Hoskam, and P. W. Brouwer, Second-order topological insulators and superconductors with an order-two crystalline symmetry, Phys. Rev. B **97**, 205135 (2018).

[44] L. Trifunovic and P. W. Brouwer, Higher-Order Bulk-Boundary Correspondence for Topological Crystalline Phases, Phys. Rev. X **9**, 011012 (2019).

[45] W. A. Benalcazar, T. Li, and T. L. Hughes, Quantization of fractional corner charge in C_n-symmetric higher-order topological crystalline insulators, Phys. Rev. B **99**, 245151 (2019).

[46] M. Ezawa, Strong and weak second-order topological insulators with hexagonal symmetry and $\mathbb{Z}_3$ index, Phys. Rev. B **97**, 241402(R) (2018).

[47] M. Ezawa, Magnetic second-order topological insulators and semimetals, Phys. Rev. B **97**, 155305 (2018).

[48] E. Khalaf, Higher-order topological insulators and superconductors protected by inversion symmetry, Phys. Rev. B **97**, 205136 (2018).

[49] D. Călugăru, V. Juričić, and B. Roy, Higher-order topological phases: A general principle of construction, Phys. Rev. B **99**, 041301(R) (2019).